Fuel 392 (2025) 134880

Contents lists available at ScienceDirect

Fuel

journal homepage: www.elsevier.com/locate/fuel

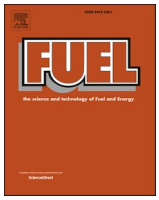

Full Length Article

Experimental study on in-furnace denitrification with iron-based additives in a circulating fluidized bed combustor

Chengliang Han, Lilin Hu, Ruifang Zhang, Yang Zhang, Junfu Lyu, Hai Zhang *

Key Laboratory for Thermal Science and Power Engineering of Ministry of Education, Department of Energy and Power Engineering, Tsinghua University, Beijing, China

ARTICLE INFO

Keywords:
Circulating fluidized bed
Iron-based additives
Combustion
De-NOx

ABSTRACT

Circulating fluidized bed (CFB) coal combustion technology has advantages of excellent fuel flexibility, wide turn-down ratio, as well as the effective-cost control on SO_2 and NOx emissions. As the emission standard becomes more and more stringent, new technologies to further reduce the original pollutant are desired. In this work, an in-furnace denitrification technology for CFB coal combustion using iron-based additives was proposed and experimentally assessed in an apparatus with a riser taller than 20 m. The tall CFB rig ensured coal particles to experience a chemical process like those burnt in a practical CFB boiler, with a compatible burnt-out rate and O_2 content at the exit. Iron particles with an average size close to that of quartz sand bed materials were used as the initial additives. Results showed that when 10 % of iron powders with respect to the mass of the initial bed inventory was added, the iron-based additives were mainly in the middle and lower parts of the riser. The emission of NO could be reduced by 9.4 % − 27 %, and the total amount of N-containing pollutants (NO + N_2O) could be reduced by 8.1 % − 9.2 %. At the same time, CO concentration in the exhaust gas decreased by 4.9 % − 38.1 %. The variation degrees depended on the combustion temperature and the air staging. However, the presence of iron additives was in favor of decreasing N_2O emission, it did not always decrease NO emission. In some cases, it could even increase NO emission, when combustion occurred in an oxidizing atmosphere. The results showed that the proposed in-furnace denitrification technology with iron additives for CFB coal combustion was feasible for the total nitrogen oxide removal, but conditional in NO reduction. To achieve the simultaneous NOx and N_2O reduction, proper control of additive size, bed temperature and reaction atmosphere should be performed.

1. Introduction

Circulating fluidized bed (CFB) coal combustion technology has been widely used in power generation due to its advantages of excellent fuel flexibility, wide turn-down ratio [1,2], as well as the effective-cost control on SO_2 and NOx emissions [3,4]. The low NOx emission is attributed to the moderate temperature combustion (800 ~ 900 ℃), an overall reducing dense bed and a large amount of unburnt char in the combustor, and the existence of catalytic metal oxides in coal ash [5–7]. Though several applications showed that with the fine circulating particles and proper combustion organization, the NOx emission at the exit of a CFB boiler could be controlled at less than 50 mg/m^3 (@6% O_2, hereafter the same) [8,9], there are still many coal-fired CFB boilers operating with rather high NOx emission. Therefore, in many cases, the expensive selective catalytic reduction (SCR) [10] or rather expensive selective non-catalytic reduction (SNCR) [11] measures still have to used for flue gas treatment. These measures bring not only extra cost, but also the ammonia (NH_3) slip especially when a CFB boiler operates at low loads [12]. The NH_3 slip could cause a secondary environmental pollution, and the corrosion and blockage in the air preheater as well [13]. Therefore, it is of great interest to assess the feasibility to develop an economical, NH_3-free, in-furnace denitrification technology with additives for coal-fired CFB boilers.

Iron and iron oxides, as common components in the coal ash and rich in natural resource, are inevitably regarded as the potential additives. Indeed, several studies have been conducted on the NO and N_2O reduction with the presence of iron and iron oxides. Hayhurst et al. [14,15] experimentally found iron has a strong catalytic effect on NO and N_2O reduction in a fluidized bed in a reducing atmosphere. Zhou et al. [16] used thermogravimetric analysis (TGA) to assess the chemical reactions between iron and its oxides with N_2O and NO in the presence of CO at fluidized bed combustion temperatures, and found iron

* Corresponding author.
E-mail address: haizhang@tsinghua.edu.cn (H. Zhang).

https://doi.org/10.1016/j.fuel.2025.134880
Received 14 April 2024; Received in revised form 18 February 2025; Accepted 25 February 2025
Available online 4 March 2025

effectively decreased the decomposition temperature of N_2O, and with the presence of CO, iron could reduce part of NO and N_2O [16]. Recently, a few studies further confirmed that in the presence of CO, iron and iron oxides can effectively reduce NOx, and play a role of catalyst. The experimental results of Lyu et al. [17] showed that iron oxides experience occurrence transformation and different occurrence has different NO reduction performance with CO in the fluidized bed combustion temperature. F_2O_3 barely reacts with NO. However, F_2O_3 can be reduced by CO into FeO or Fe_3O_4, and the produced FeO or Fe_3O_4 can catalyze the NO reduction reaction with CO. In a CFB boiler, the iron oxides in the circulating ash are mainly Fe_3O_4 [18]. Thus, Hu et al. [18,19], by quantum computing with density functional theory (DFT) revealed that NO absorbed onto Fe_3O_4 surface to form $(NO)_2$ dimer structure is a possible pathway for the reduction of NO by CO over Fe_3O_4 [19,20]. However, the presence of O_2, namely an oxidizing atmosphere can prevent the NO reduction with CO [21,22].

Based on the previous studies, obvious catalytic effect of iron oxides on the reaction of CO and NO could exist under a reducing atmosphere condition. By coincidence, as found the previous studies [6,11] the dense bed of a CFB boiler is in an overall reducing atmosphere, and there exists abundant CO. Thus, if the iron oxides could be remained in the dense bed region, NOx could be cost-effectively reduced in the furnace of a coal-fired CFB boiler. Due to the complexity of the CFB coal combustion, the feasibility assessment of the proposed technology should not limited to a fixed bed, TGA and small size fluidized bed experiments. Especially, a tall CFB combustor is essential to ensure the coal particles in the riser experience a similar chemical process as those burnt in a CFB boiler, with the similar burnt-out rate and O_2 content at the combustor exit.

Consequently, an experimental study was carried out to assess the effectiveness and conditions for the in-furnace de-NOx method using iron-based additives for CFB combustion. The experiments were conducted in an easy-controlled small capacity (~30 kW fuel input) coal-fired CFB combustor but with the riser taller than 20 m. NOx emissions with the iron-based addition were detected under different air-staging conditions. The ash samples were also analyzed. The experimental results were discussed to explored the influencing factors.

2. Experimental approach

2.1. CFB combustor with the height of 20 m

Fig. 1 shows the schematic of the experimental system of the tested CFB apparatus with a thermal capacity of 30 kW. The system consisted of a combustor unit, a heating furnace unit, a feeding unit, a flue gas cooling and cleaning unit, a gas supplying unit, and a data acquisition unit.

The main part of the CFB combustor was a riser with a net height of 22 m. Such a tall riser allowed coal particles in the riser experience a similar chemical process as those in a CFB boiler. The lower part of the riser was 120 mm in diameter for the convenience to form a dense bed, and the rest was 98 mm in diameter. At the exit of the riser, there was a highly efficient cyclone, used for gas–solid separation. At the end of the standard pipe, there was a loop seal used for returning the solid particles to the riser.

The riser, cyclone, leap seal and pipes were made of stainless steel. They were enclosed by a box-type electrical heater. The heater has six sections and the temperature of each section could be independently controlled. Before the experiments, the CFB loop was heated to a preset temperature.

The test coal was fed into the riser by a screw feeder, placed outside of the heater box, at a height of ~ 300 mm from the air distributor. The primary air was introduced through air distributor placed on the bottom of the riser and the secondary air ports were located at two levels with the elevation of 1000 mm and 2000 mm from the air distributor, respectively. The solids collected by the cyclone were stored in the standpipe and then returned to the lower part of the riser through a loop seal. Before released into the atmosphere, the flue gas was cooled by a heat exchanger and then cleaned by a bag filter.

The data acquisition unit acquired temperature, flow rate, and concentrations of flue gas components, etc. Temperature was measured at more than 20 locations along the ash circulating loop. The

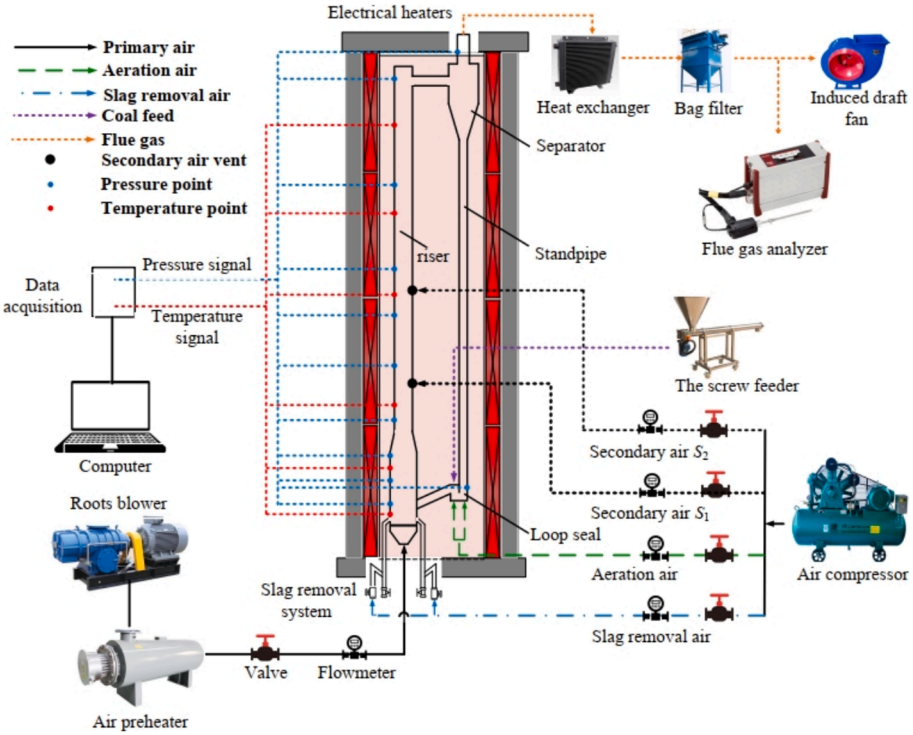

Fig. 1. Schematic diagram of the electrical-heating CFB apparatus with riser taller than 20 m.

thermocouples used in the experiment were WRNK-291 armored ones. with measurement range of 0–1100 °C. The allowable deviation of the thermocouples was 0.5 % of the measured temperature. The flow rates of gas were measured by flow meters. The ash sampling ports were located at the bottom of the riser and the loop seal. The concentrations of O_2, CO_2, CO, SO_2, NO, and N_2O in the flue gas were continuously monitored by online gas analyzers placed before the bag filter.

2.2. Fuel and bed materials

A Chinese Liulin bituminous coal (LL) was tested. The proximate and ultimate analyses at as-received base are listed in Table 1. The coal was sieved to 0——2 mm. Quartz sand was used as the bed material with an initial bed inventory of 12 kg. 10 % of iron powders with respect to the initial bed inventory were used as iron-based additives. The addition ratio of iron-based additive was 10 % of the initial bed inventory, and the high-purity iron powder was used, with a purity of more than 99 %. In the combustion experiment, iron powder reacted with oxygen to form iron oxides, a mixture of Fe_2O_3 and Fe_3O_4. A Fe_3O_4 molecule can be regarded as a Fe_2O_3 unit (where iron is in the + 3 oxidation state) and a FeO unit (where iron is in the + 2 oxidation state), that is, the chemical formula can be expressed as Fe_2O_3·FeO, which indicates that a FeO unit is embedded in the structure of Fe_2O_3. With sufficient oxygen and time, at a high temperature, Fe_3O_4 would be fully converted into more stable Fe_2O_3 [22]. The particle size distributions of quartz sand and iron powders are shown in Fig. 2, with the average particle sizes ($\bar{d}_p$ J) of 108 μm and 98 μm respectively.

The main compositions of coal ash were analyzed using X-ray fluorescence spectroscopy (XRF), and the results are shown in Table 2. The main components of coal ash are oxides of Si, Al, Fe, Ca, and Ti, of which the content of SiO_2 and Al_2O_3 accounts for more than 70 %. The iron content is 5.58 %.

2.3. Test conditions

When the experiment started, the CFB combustor with a certain amount of bed material was heated up in a programmed rate to a preset temperature. Then, the primary air was preheated by a gas preheater to more than 300 °C and then introduced to the air distributor at a given flow rate. After the bed material circulation was built up and the riser reached the preset bed temperature, the test coal was fed into the combustor by a screw feeder with a pre-calibrated feeding rate. After the combustion was stable, the iron-based additives were added to the bottom of the riser. During the experiments the flue gas composition was measured online by a gas analyzer. After the experiment, the bottom ash was discharged from the riser and the loop seal.

In order to assess the effect of air staging on NOx emission characteristics under the presence of iron-based additives, experiment 1 (Exp 1) and experiment 2 (Exp 2) were designed respectively. In both experiments, when stable combustion was first achieved without the secondary air, about 1.2 kg of iron-based additives were sent into the bottom of the riser. After the outlet flue gas concentration was stable, the lower secondary air (S_1) was introduced. To keep the total air flow rate unchanged, the flow rate of the primary air (Q_r) was reduced accordingly. The difference between the two experiments was in Exp1 the lower secondary air (S_1) was fully switched to the upper secondary air (S_2), while in Exp2, only 40 % S_1 was replaced by S_2. In the experiment, the coal feeding rate G was controlled at 6.45 kg/h. The temperatures of dense bed and dilute phase were controlled at 750 °C. The other parameters, including Q_r, S_1, and S_2 are shown in Table 3.

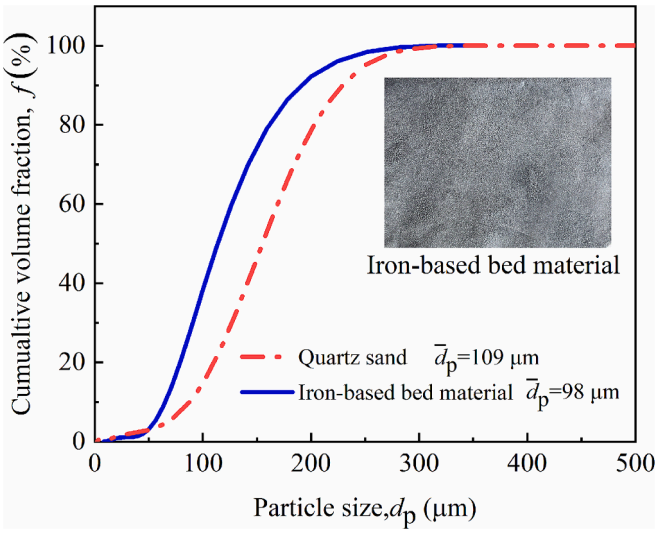

Fig. 2. Particle size distribution of sand and iron powders.

Table 2
Composition of the ash for the used coal, unit:%.

SiO_2	Al_2O_3	Fe_2O_3	CaO	TiO_2	K_2O	Na_2O	MgO
43.32	42.46	5.58	2.91	1.80	0.57	0.34	0.24

3. Results and discussion

3.1. Temperature distributions

Fig. 3 depicts the temporal temperature variations at various heights of the riser and the bottom of the downpipe for Exp 1. It can be seen that before coal is fed into the furnace, the measured temperatures keep rising as the entire system is electrically heated up. When the dense bed temperature reach to 550°C, coal is fed in. Then, all the measured temperatures rise quickly to 700 ~ 850 °C. If the measured temperature is lower than the preset temperature of 750 °C, the corresponding session is still electrically heated.

It can be seen there is some difference between the upper and lower riser temperatures. Before the coal is added in, the measured temperature increases along the riser height. This is due to the larger thermal inertia and strong heat loss in the lower riser. After the coal is fed in, temperatures in the lower riser increase much faster and reach a higher

Table 3
The experimental conditions.

Item	Exp1	Exp2
Coal feeding rate,G (kg/h)	6.45	6.45
Initial bed temperature, T (°C)	750	750
Initial bed inventory, I_v (kg)	12	12
The mass of iron-based additives, m (kg)	1.2	1.2
Primary air flow, Q_r (Nm^3/h)	19.8	15.8
Lower secondary air flow, S_1 (Nm^3/h)	0/5/0	0/5/3
Upper secondary air flow, S_2 (Nm^3/h)	0/0/5	0/0/2

Table 1
Proximate and ultimate analyses of the test coal.

Proximate analysis, wt.%				Ultimate analysis, wt.%					Lower heating value/kJ·kg^{-1}
FC_{ar}	V_{ar}	A_{ar}	M_{ar}	C_{ar}	H_{ar}	O_{ar}	N_{ar}	S_{ar}	Q_{ar}
53.84	16.72	28.87	0.57	62.93	2.8	0.59	0.72	3.52	24384.35

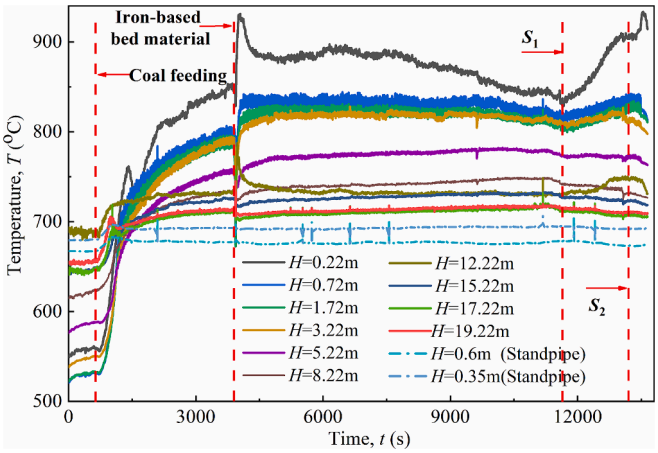

Fig. 3. Axial temperature distribution for the Exp 1.

value than those in the upper riser, indicating that coal is mostly burn in the dense bed region. When the iron particles are added, the bed temperature increases rapidly, particularly in the lower riser. This is due to the fast heat release from the oxidization of the iron powder with $\overline{d}_p$ of 98 μm at a high temperature of ~ 800 °C. When the oxidization reaction ends, the temperature gradually falls down to the original level. Then when the secondary air S_1 or S_2 are supplied, the bed temperature rises again. Apparently, there is a certain fluctuation of the measured temperatures induced by the nature of gas–solid flow. The most unstable temperature variation happens at the lowest measuring point. The results indicate that many of iron and iron oxide particles stay in the bottom riser while subjected to a complex fluidization status.

Fig. 4 depicts the bed temperature distributions along the riser at stable operation under different experimental conditions. The temperature at the bottom riser is in the range of 800 ~ 968 °C, which is higher than that at the upper part (at a value of ~ 750 °C), confirming that coal combustion mainly occurs there. The addition of the secondary air and iron-based additives increases the bed temperature.

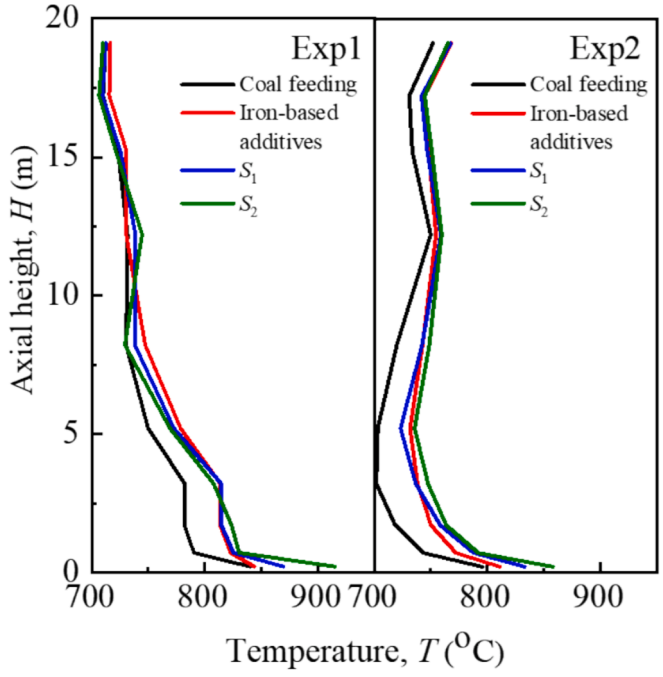

Fig. 4. Axial distributions of bed temperature under different experimental conditions.

The effect on bed temperature by iron-based additives could be attributed to three aspects. Firstly, the added iron particles can be oxidized into iron oxides through a strong exothermic reaction. Secondly, iron and iron oxides could play a catalytic role to accelerate the fuel combustion process and change the combustion reaction path. Thus the fuel burns more completely and efficiently [23–25], and some exothermic reactions more prominent [24,26,27]. Thirdly, iron particles might also increase the overall thermal conductivity of the bed materials, resulting in more even temperature distribution in the combustion chamber, thereby increasing the overall temperature [24,25,28].

The bed temperature rise induced by the introduction of the secondary air could be also attributed to a few factors. Firstly, the enhancement of the mixing of fuel and oxygen. The increased secondary air flow rate could improve the O_2 distribution in the combustion zone, promoting a more complete burnt-out and there more heat release [29]. Meanwhile, the high-speed secondary air effectively dispersed combustion products, improved the O_2 diffusion and enhanced the combustion process [30–33]. In addition, the secondary air enhanced the heat transfer in the combustion zone, resulting in more uniform temperature distribution and a higher bed temperature [30].

3.2. Flue gas composition

Fig. 5(a) shows the temporal variations of the O_2 concentration of flue gas in Exp 1. The O_2 concentration is in the range of 4.5 % ~ 5.2 % during stable combustion. Right after adding the iron powders, it rises suddenly and then decreases sharply. The sudden rise may be due to the leak of some air during the addition of the additives. As O_2 reacts with the iron powders, its concentration decreases sharply. As iron powders are oxidized, O_2 rebounds slowly back. The addition of staging air S_1 promotes the combustion of coal, and O_2 is further reduced. However, the position of staging air S_2 is rather high, so that the coal combustion is incomplete, increasing the O_2 concentration. Fig. 5(b) depicts the temporal variations of N-containing pollutants in flue gas for Exp 1. The flue gas concentrations were converted into 6 % O_2 base ones and compared with the average value.

3.2.1. Temporal variations of N-containing pollutants

To reveal the trend of concentration change more clearly, the temporal variation of the average concentration fluctuation of N-containing pollutants (NO + N_2O).is depicted in Fig. 6. Without the addition of iron-based additives, the average NO concentration at the furnace outlet is

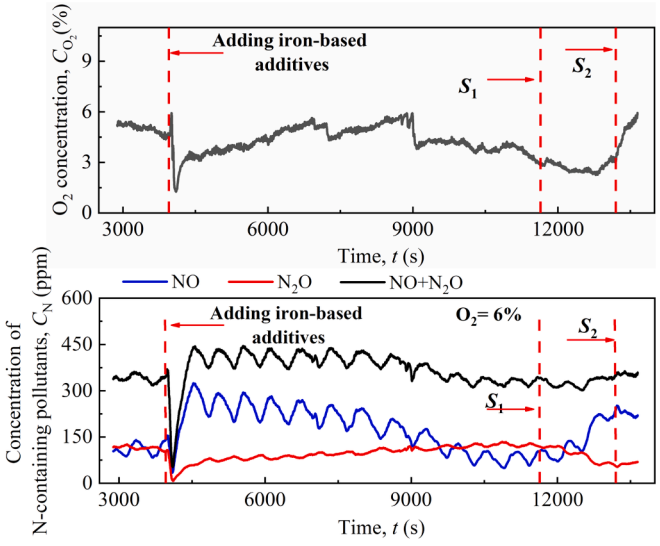

Fig. 5. Temporal variations of flue gas composition in Exp1(a: O_2; b: nitrogen oxides).

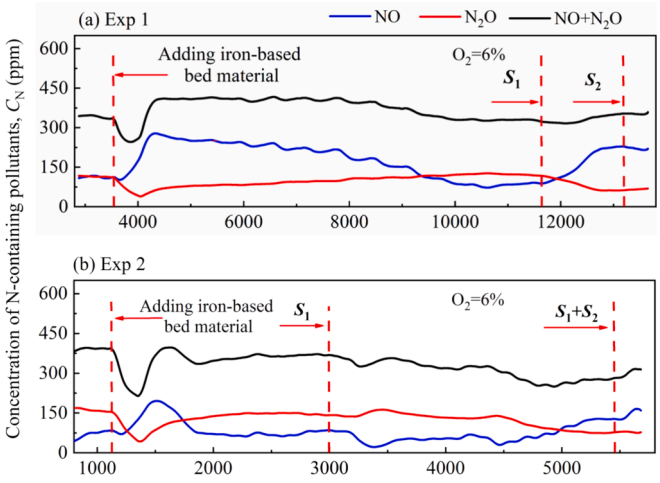

Fig. 6. The temporal variations of N-containing pollutants during the experiments.

between 70—110 ppm. After additives are added, the average NO concentration increases and then decreases. Because the added iron powders preferentially consume a certain amount of O_2, the coal combustion is weakened. When the iron additives are mostly oxidized, a large portion of coal is burned, causing increase of the temperature and NO formation. When the coal is burned out, NO emission gradually decreases and finally reaches stable.

3.2.2. Temporal variations of CO and SO_2 pollutants

Fig. 7 shows the measured CO and SO_2 concentrations in the flue gas. The CO concentration is between 500 ~ 1600 ppm. The SO_2 concentration is 1500 ~ 2000 ppm, which is due to the high sulfur content in LL coal. After iron additives are added, the CO concentration increases and then decreases, but the SO_2 concentration varies oppositely. Because the added iron additives preferentially consume a certain amount of O_2, the coal combustion is weakened, resulting in an increase in CO and a decrease in SO_2. When the iron additives are mostly oxidized, a large portion of coal is burned, causing CO to decrease and SO_2 to increase.

3.3. Effect of iron-based additives on flue gas concentrations without air staging

Fig. 8 compares the flue gas concentrations without and with iron-based additives when no air staging is used. With the iron-based additives, CO concentration in the flue gas decreases by 4.9 % – 38.9 % and the SO_2 concentration decreases by 5 % – 5.5 %. In the same time, NO concentration decreases by 9.4 % – 27 %. The total amount of N-containing pollutants (NO + N_2O) decreases by 8.1 % – 9.2 %, indicating that some nitrogen oxides are converted into N_2.

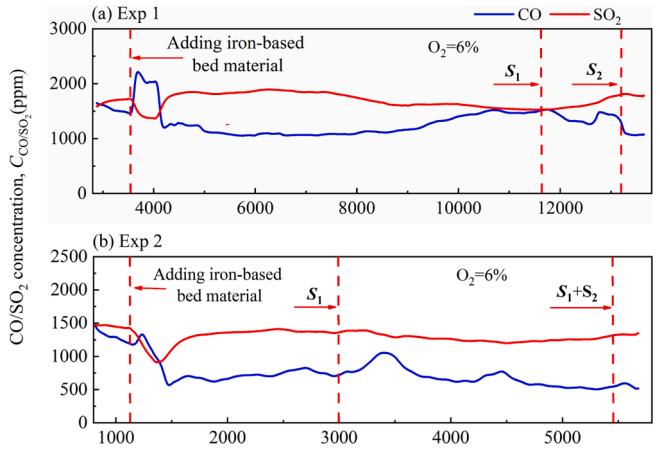

Fig. 7. The temporal variations of CO and SO_2 during the experiments.

3.4. De-NOx effect with iron-based additives under air staging

Fig. 9 shows the impact of the air staging on denitrification in CFB with iron-based additives. After adding the secondary air streams S_1 or S_2, the NO concentration increases, but the N_2O concentration decreases. The introduced secondary air significantly affects the distribution of temperature, oxygen concentration and CO concentration in the furnace. As shown in Fig. 7, the CO concentration in Exp 1 and Exp 2 decreased since the secondary air stream S_1 or S_2 causes a weaker reducing atmosphere. Previous studies [17,20] found iron oxides undergo valence transition in a fluidized bed environment. The low-valent iron oxides have high efficiency for NO removal in a reducing atmosphere but not in an oxidizing atmosphere. Thus, the NO generation could be enhanced as iron oxides are carried into the dilute bed. On the other hand, the secondary air results in a reduction of the primary air and an increase in the lower riser temperature. This is in favor to the NO reduction as the additives are kept in the lower riser. The enhancement effect in dilute zone and reduction effect in the dense bed in NO generation compete each other, resulting in a conditional overall NO reduction. The results also indicate that the fluidization behaviors of the iron-based additives play crucial effect and is recommended to be further investigated in the future.

3.5. Ash sample analysis

Fig. 10 shows the images of ash samples collected in Exp 1. The color of the ash sample directly related to its constituent elements, particularly metal elements, and the presence of unburned coal. The ash samples collected in the riser are mainly brown. This could be attributed to that in the high temperature rise, most of the iron-based additives are oxidized to rather stable Fe_2O_3, which has a unique brown color. The ash sample released from the bottom of the riser is darker, indicating that some unburned coal or carbonaceous particles exist.

Fig. 11 shows the particle size distribution of ash samples at different heights collected in Exp 1. The $\overline{d}_p$ of the ash samples gradually decreases along the riser height and it is larger than that of the initially added iron powders and quartz sand. This is because $\overline{d}_p$ of the ash samples is not only affected by the quartz sand and iron powder, but also by the coal particle. The coal particles was in the range of 0–2 mm, resulting in larger average ash particle size.

Fig. 12 shows the composition of the ash samples collected in Exp 1. The main component of the ash sample is SiO_2 as the initial bed material is quartz sand. Al_2O_3 content in fly ash is much higher than that in the riser. Provided the coal used in Exp 1 contains 42.5 % Al_2O_3, it could be inferred that a large amount of ash produced by burning coal is conveyed by the fluidizing air to and pass the separator.

The fly ash has high iron content, which may be due to the discharged of finer iron-based additives. The iron content in the middle and lower riser is similar, but significantly higher than that in the upper riser. This is determined jointly by the size of the bed material and the superficial gas velocity. Due to the high density, the coarse iron particles have large terminal velocity, so they are difficult to be carried to the upper riser under the existing fluidizing air velocity. Thus, relatively high iron content exists in the middle and lower riser. The iron content in the fly ash, however, comes from the small iron particles and the iron minerals contained in the coal. The escape of small iron-based bed material may affect the final denitrification effect. To ensure the De-NOx efficiency, it is necessary to select the appropriate particle size according to the efficiency of the separator. In addition, the SO_3 content in the ash at different locations is higher than that in the coal ash, indicating that the iron-based additives absorb part of the SO_2 and fix it in the ash.

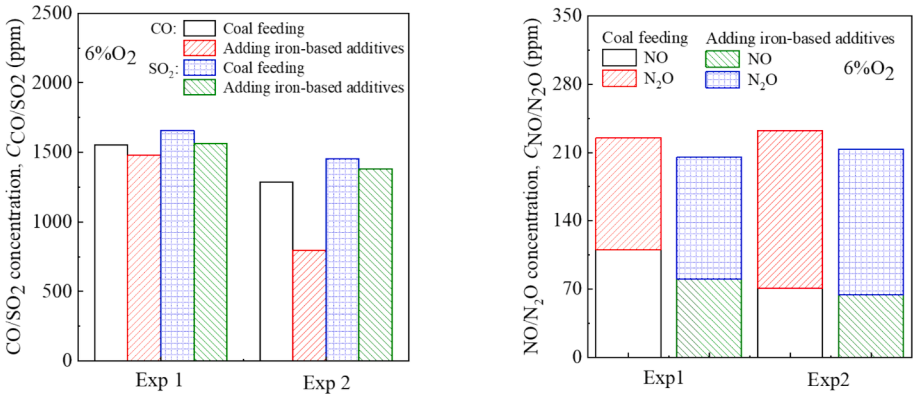

Fig. 8. Effect of iron-based additives on flue gas concentration without air staging.

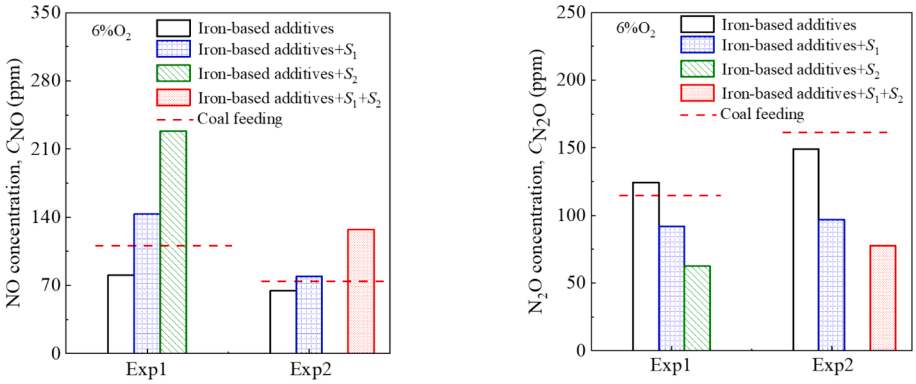

Fig. 9. De-NOx effect with iron-based additives when air staging was applied.

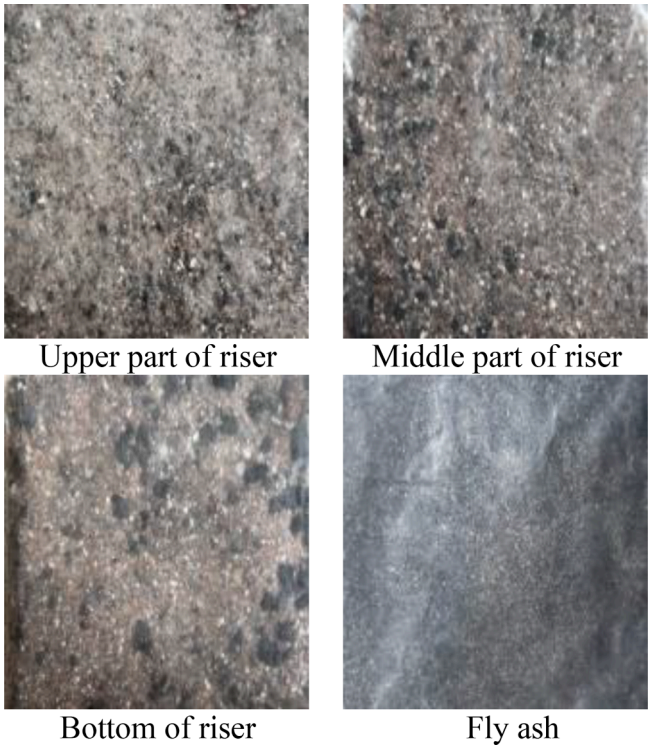

Fig. 10. Images of ash samples collected under Exp 1.

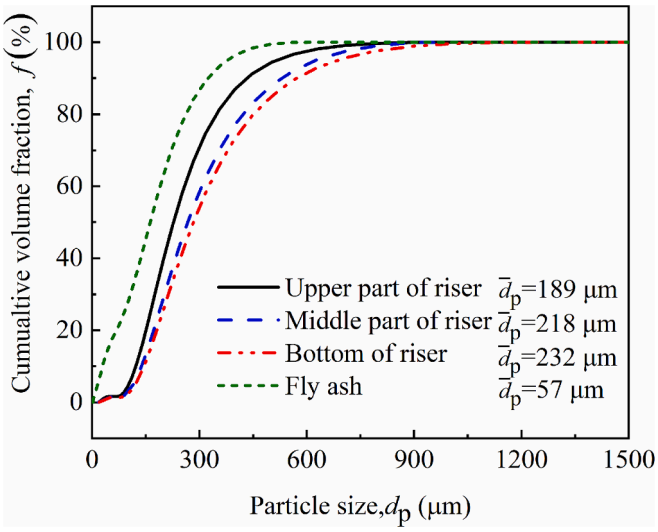

Fig. 11. The particle size distribution of collected ash samples in Exp1.

4. Conclusions

An in-furnace denitrification technology for CFB coal combustion with iron-based additives was proposed and experimentally assessed with a riser taller than 20 m. The experimental results showed that when iron particles with an average size close to that of quartz sand bed materials were used as the initial additives, and amount of 10 % of that of the initial bed inventory, the NO emission could be reduced by 9.4 % – 27 %, and the total amount of N-containing pollutants ($NO + N_2O$) could

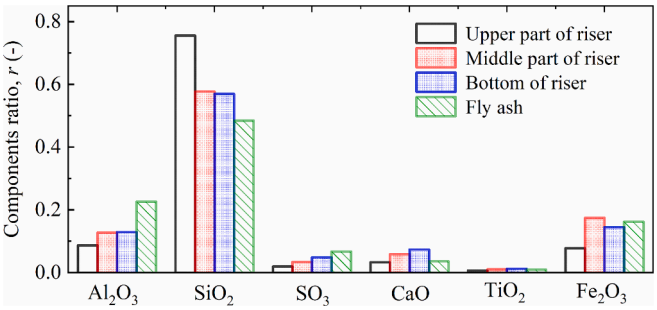

Fig. 12. Components of ash samples collected in Exp 1.

be reduced by 8.1 % – 9.2 %. In the same time, CO concentration in the exhaust gas decreased by 4.9 % – 38.1 %. The variation degrees depended on the combustion temperature and the air staging. However, the presence of iron additives was in favor of decreasing N_2O emission, it did not always decrease NO emission. In some cases, it could even increase NO emission, due to the weakening of the reducing atmosphere. The results showed that the proposed in-furnace denitrification technology with iron additives for CFB coal combustion was feasible for the total nitrogen oxide removal, but conditional in NO reduction. To achieve simultaneous NOx and N_2O reduction, proper control of additives size, bed temperature and reaction atmosphere were necessary.

CRediT authorship contribution statement

Chengliang Han: Writing – original draft, Methodology, Investigation. **Lilin Hu:** Writing – original draft, Methodology, Investigation. **Ruifang Zhang:** Methodology, Investigation. **Yang Zhang:** Writing – review & editing, Supervision, Methodology, Investigation. **Junfu Lyu:** Validation, Project administration, Conceptualization. **Hai Zhang:** Writing – review & editing, Supervision, Funding acquisition, Conceptualization.

Declaration of competing interest

The authors declare that they have no known competing financial interests or personal relationships that could have appeared to influence the work reported in this paper.

Acknowledgment

This work was financially supported by the Chinese National Key Development Project (2020YFB0606303) and Chinese National Natural Science Foundation project (NSCF #U1710251).

Data availability

Data will be made available on request.

References

[1] Feng J, Yue G, Lyu J. Circulating fluidized bed combustion boiler[M] (in Chinese). Beijing: Electric Power Industry Press; 2003.
[2] Basu P. Circulating fluidized bed boilers: design, operation and maintenance[M]. 1st ed. Halifax: Springer; 2015.
[3] Johnsson JE. Formation and reduction of nitrogen oxides in fluidized-bed combustion [J]. Fuel 1994;73(9):1398–415.
[4] Leckner B. Fluidized bed combustion: mixing and pollutant limitation [J]. Prog Energy Combust Sci 1998;24:31–61.
[5] Yue G, Lyu J, Zhang H, et al. Design Theory of circulating fluidized bed boilers [R], in: Proceedings of 18th International Conference on Fluidized Bed Combustion, Toronto, Canada, May 22-25, 2005, pp. 18 29.
[6] Yue G, Cai R, Lu J, et al. From a CFB reactor to a CFB boiler–The review of R&D progress of CFB coal combustion technology in China [J]. Powder Technol 2017;316:18–28.
[7] Cai R, Zhang H, Zhang M, et al. Development and application of the design principle of fluidization state specification in CFB coal combustion [J]. Fuel Process Technol 2018;174:41–52.
[8] Ke X, Cai R, Zhang M, et al. Application of ultra-low NOx emission control for CFB boilers based on theoretical analysis and industrial practices [J]. Fuel Process Technol 2018;181:252–8.
[9] Zhang H, Lyu J, Yue G. A review on research and development of CFB combustion technology in China [J]. Powder Technol 2023;414:118090.
[10] Zhao S, Peng J, Ge R, et al. Research progress on selective catalytic reduction (SCR) catalysts for NOx removal from coal-fired flue gas [J]. Fuel Process Technol 2022;236:107432.
[11] Ke X, Engblom M, Yang H, et al. Prediction and minimization of NOx emission in a circulating fluidized bed combustor: A comprehensive mathematical model for CFB combustion [J]. Fuel 2022;309:122133.
[12] Cheng X, Cheng Y, Wang Z, et al. Comparative study of coal based catalysts for NO adsorption and NO reduction by CO [J]. Fuel 2018;214:230–41.
[13] Yao X, Zhang M, Kong H, et al. Investigation and control technology on excessive ammonia-slipping in coal-fired plants [J]. Energies 2020;13(16):4249.
[14] Hayhurst AN, Lawrence AD. The reduction of the nitrogen oxides NO and N_2O to molecular nitrogen in the presence of iron, its oxides, and carbon monoxide in a hot fluidized bed [J]. Combust Flame 1997;110(3):351–65.
[15] Hayhurst AN, Ninomiya Y. Kinetics of the conversion of NO to N_2 during the oxidation of iron particles by NO in a hot fluidised bed [J]. Chem Eng Sci 1998;53(8):1481–9.
[16] Zhou H, Lu J, Zhou H. The reduction of nitrogen oxides N_2O/NO in the presence of Fe, its oxides, and CO in fluidized bed combustion of coal [J]. Proceedings Chinese Society of Electrical Engineering (in Chinese) 2001;21:44–7.
[17] Lyu J, Hu L, Song T, et al. Occurrence transformation of iron oxides and their catalytic reduction of NO under fluidized bed temperature and CO[J]. Chemical Industry and Engineering Progress (in Chinese) 2020;39(11):4474–9.
[18] Hou X, Zhang H, Yang S, et al. N_2O decomposition over the circulating ashes from coal-fired CFB boilers[J]. Chem Eng J 2008;140(1–3):43–51.
[19] Hu L, Zhang Y, Liu Q, et al. Density Functional Theory Study on the Reduction of NO by CO Over Fe3O4 (111) Surface [J]. Combust Sci Technol 2022:1–14.
[20] Hu L, Zhang Y, Zhang H, et al. Catalytic reduction of NO by CO over Fe-doped penta-graphene as a promising catalyst: A density functional study [J]. Mol Catal 2020;496:111194.
[21] Cheng X, Wang L, Wang Z, et al. Catalytic performance of NO reduction by CO over activated semicoke supported Fe/Co catalysts [J]. Ind Eng Chem Res 2016;55(50):12710–22.
[22] Li L, Mao J, Tang W, et al. Experimental study on coal combustion by using the ilmenite ore as active bed material in a 0.3 MWth circulating fluidized bed [J]. Fuel 2023;342:127007.
[23] Xu S, Xu L, Bai X, et al. Phase change and combustion of iron particles in premixed $CH_4/O_2/N_2$ flames [J]. Combust Flame 2024;259(Jan.):1.1-1.8.
[24] Cai X, Zhang L, Wang J, et al. Analysis of combustion characteristics and product morphology of single iron particle [J]. CIESC Journal 2023;74(11):4702–9.
[25] Li S, Huang J, Weng W, et al. Ignition and combustion behavior of single micron-sized iron particle in hot gas flow [J]. Combust Flame 2022;241:112099.
[26] Choisez L, Rooij N, Hessels C, et al. Phase transformations and microstructure evolution during combustion of iron powder [J]. Acta Mater 2022;239:118261.
[27] Mich J, Braig D, Gustmann T, et al. A comparison of mechanistic models for the combustion of iron microparticles and their application to polydisperse iron-air suspensions [J]. Combust Flame 2023;256:112949.
[28] Thijs L, Gool C, Ramaekers W, et al. Resolved simulations of single iron particle combustion and the release of nano-particles [J]. Proc Combust Inst 2023;39:3551–9.
[29] Yan J, Lu X, Wang Q, Kang Y, et al. Study on the influence of secondary air on the distributions of flue gas composition at the lower part of a 600 MW supercritical CFB boiler [J]. Fuel Process Technol 2019;196.
[30] Song M, Zeng L, Zhao Y, et al. Secondary air distribution in a 600 MWe multi-injection multi-staging down-fired boiler: A comprehensive study [J]. J Energy Inst 2020;93:1250–60.
[31] Zhang X, Chen Z, Jiang G, et al. Effect of central secondary air on flow and combustion characteristics of 600-MWe down-fired boiler: From laboratory to industrial site [J]. Fuel 2022;330:125677.
[32] Ersoy LE, Golriz MR, Koksal M, et al. Circulating fluidized bed hydrodynamics with air staging: an experimental study [J]. Powder Technol 2004;145(1):25–33.
[33] Zheng W, Zhang M, Zhang Y, et al. The effect of the secondary air injection on the gas–solid flow characteristics in the circulating fluidized bed [J]. Chem Eng Res Des 2019;141:220–8.